Special Issue

Optical Coherence Tomography Angiography Vessel Density in Healthy, Glaucoma Suspect, and Glaucoma Eyes

Adeleh Yarmohammadi,[1] Linda M. Zangwill,[1] Alberto Diniz-Filho,[1,2] Min Hee Suh,[1,3] Patricia Isabel Manalastas,[1] Naeem Fatehee,[1] Siamak Yousefi,[1] Akram Belghith,[1] Luke J. Saunders,[1] Felipe A. Medeiros,[1] David Huang,[4] and Robert N. Weinreb[1]

[1]Hamilton Glaucoma Center, Shiley Eye Institute, Department of Ophthalmology, University of California, San Diego, La Jolla, California, United States
[2]Department of Ophthalmology and Otorhinolaryngology, Federal University of Minas Gerais, Belo Horizonte, Brazil
[3]Department of Ophthalmology, Haeundae Paik Hospital, Inje University College of Medicine, Busan, South Korea
[4]Casey Eye Institute, Oregon Health & Science University, Portland, Oregon, United States

Correspondence: Robert N. Weinreb, Hamilton Glaucoma Center, Department of Ophthalmology, University of California, San Diego, 9500 Gilman Drive, La Jolla, CA, 92093-0946, USA;
rweinreb@ucsd.edu.

AY and LMZ are joint first authors.

Submitted: December 14, 2015
Accepted: March 29, 2016

Citation: Yarmohammadi A, Zangwill LM, Diniz-Filho A, et al. Optical coherence tomography angiography vessel density in healthy, glaucoma suspect, and glaucoma eyes. *Invest Ophthalmol Vis Sci*. 2016;57:OCT451–OCT459.
DOI:10.1167/iovs.15-18944

Purpose. The purpose of this study was to compare retinal nerve fiber layer (RNFL) thickness and optical coherence tomography angiography (OCT-A) retinal vasculature measurements in healthy, glaucoma suspect, and glaucoma patients.

Methods. Two hundred sixty-one eyes of 164 healthy, glaucoma suspect, and open-angle glaucoma (OAG) participants from the Diagnostic Innovations in Glaucoma Study with good quality OCT-A images were included. Retinal vasculature information was summarized as a vessel density map and as vessel density (%), which is the proportion of flowing vessel area over the total area evaluated. Two vessel density measurements extracted from the RNFL were analyzed: (1) circumpapillary vessel density (cpVD) measured in a 750-μm-wide elliptical annulus around the disc and (2) whole image vessel density (wiVD) measured over the entire image. Areas under the receiver operating characteristic curves (AUROC) were used to evaluate diagnostic accuracy.

Results. Age-adjusted mean vessel density was significantly lower in OAG eyes compared with glaucoma suspects and healthy eyes. (cpVD: 55.1 ± 7%, 60.3 ± 5%, and 64.2 ± 3%, respectively; $P < 0.001$; and wiVD: 46.2 ± 6%, 51.3 ± 5%, and 56.6 ± 3%, respectively; $P < 0.001$). For differentiating between glaucoma and healthy eyes, the age-adjusted AUROC was highest for wiVD (0.94), followed by RNFL thickness (0.92) and cpVD (0.83). The AUROCs for differentiating between healthy and glaucoma suspect eyes were highest for wiVD (0.70), followed by cpVD (0.65) and RNFL thickness (0.65).

Conclusions. Optical coherence tomography angiography vessel density had similar diagnostic accuracy to RNFL thickness measurements for differentiating between healthy and glaucoma eyes. These results suggest that OCT-A measurements reflect damage to tissues relevant to the pathophysiology of OAG.

Keywords: glaucoma, OCT angiography, RNFL

The potential role of the microvasculature and blood flow in the pathophysiology of glaucoma, a progressive optic neuropathy[1], has been debated and extensively investigated.[2–10] Previous studies have demonstrated reduced ocular blood flow in optic nerve head, retina, choroid, and retrobulbar circulations in glaucoma.[5,7,9,11–19] However, the lack of a reproducible and relevant in vivo quantitative assessment method has limited the study of both ocular perfusion[11,20] and their microvascular networks.

Radial peripapillary capillaries (RPCs) comprise a distinct network of capillary beds located within the retinal nerve fiber layer (RNFL) that supply the retinal ganglion cell (RGC) axons.[21–24] Although histologic studies highlighted the importance of the RPC networks in glaucoma,[25–27] in vivo investigations have been limited by the lack of a technique to quantitatively characterize the microvasculature.[28] A reliable clinical method for imaging these vascular beds would improve our knowledge about the role of RPCs in RGC axonal health and disease.[29]

In this regard, optical coherence tomography angiography (OCT-A) is a new imaging modality that can be used to characterize vasculature in various retinal layers,[30] providing quantitative assessment of the microcirculation in the optic nerve head[31,32] and peripapillary region.[33] The objective of the current study is to assess the performance of OCT-A retinal vessel density measurements for differentiating among healthy subjects, glaucoma suspects, and glaucoma patients and also to compare its diagnostic accuracy to spectral-domain (SD)-OCT RNFL thickness measurements.

Methods

Study Population

This was an observational cohort study of healthy subjects, glaucoma suspects, and open-angle glaucoma (OAG) patients enrolled from the Diagnostic Innovations in Glaucoma Study

(DIGS) who completed OCT-A imaging (AngioVue; Optovue, Inc., Fremont, CA, USA)[30,31,33,34] and optic nerve head imaging using SD-OCT (Avanti; Optovue, Inc.).

The DIGS protocol and eligibility criteria have been described in detail previously.[35] In brief, all participants underwent an ophthalmologic examination, including assessment of best-corrected visual acuity, slit-lamp biomicroscopy, intraocular pressure (IOP) measurement with Goldmann applanation tonometry, gonioscopy, ultrasound pachymetry, dilated fundus examination, simultaneous stereophotography of the optic disc, and visual field testing. Inclusion criteria were (1) greater than 18 years of age, (2) open-angles on gonioscopy, and (3) best-corrected visual acuity (BCVA) of 20/40 or better.

Healthy subjects had (1) IOP <21 mm Hg with no history of elevated IOP; (2) normal appearing optic disc, intact neuroretinal rim, and RNFL; and (3) a minimum of two reliable normal visual fields, defined as a pattern standard deviation (PSD) within 95% confidence limits and a glaucoma hemifield test (GHT) result within normal limits. Eyes were classified as glaucomatous if they had repeatable glaucomatous visual field damage defined as a GHT outside normal limits and PSD outside 95% normal limits. Glaucoma suspects were defined as having glaucomatous optic neuropathy or suspicious appearing optic discs based on stereophotograph reviewed by two experienced graders and/or ocular hypertension (IOP > 21 mm Hg) without evidence of repeatable glaucomatous visual field damage. The diagnostic category for each participant was determined based on the diagnosis of his or her worse eye.

Participants with a history of intraocular surgery (except for uncomplicated cataract surgery or glaucoma surgery), coexisting retinal pathologies, nonglaucomatous optic neuropathy, uveitis, or ocular trauma were excluded from the study. Participants were also excluded if there was a diagnosis of Parkinson's disease, Alzheimer's disease, dementia, or a history of stroke. Participants with systemic hypertension and diabetes mellitus were included unless they were diagnosed with diabetic or hypertensive retinopathy. Participants having unreliable visual field, poor quality OCT-A, or optic nerve head SD-OCT scans were also excluded from our study.

Systemic measurements included two blood pressure (BP) measurements obtained using an Omron Automatic (Model BP791IT; Omron Healthcare, Inc., Lake Forest, IL, USA) blood pressure instrument. Mean arterial pressure was calculated as one-third systolic BP + two-thirds diastolic BP. Mean ocular perfusion pressure (MOPP) was defined as the difference between two-thirds of mean arterial pressure and IOP. Optical coherence tomography angiography and SD-OCT images were obtained by the same operator and at the same visit using the AngioVue, which is a dual modality OCT system. The AngioVue is an angiographic platform implemented on an existing commercially available SD-OCT platform. The AngioVue imaging system is able to provide structural measurements and vascular measurements.

Informed consent was obtained from all participants, and all methods adhered to the tenets of the Declaration of Helsinki and the Health Insurance Portability and Accountability Act and were approved by the Institutional Review Boards at the University of California San Diego.

Standard Automated Perimetry

Standard automated perimetry visual field tests were completed using Swedish Interactive Threshold Algorithm standard 24-2 (Humphrey Field Analyzer; Carl Zeiss Meditec, Dublin, CA, USA) strategies. The quality of the visual fields was reviewed by the Visual Field Assessment Center (VisFACT) staff. Only reliable tests (≤33% fixation losses and false-negative errors and ≤15% false-positive errors) and visual fields without rim and eyelid artifacts, evidence of inattention or fatigue effects, and no evidence that the abnormal results of the visual field were caused by a disease other than glaucoma, were included. Visual field result was considered to be abnormal if a GHT was outside of normal limits or a PSD fell outside of the 95% normal confidence limits.

Optical Coherence Tomography Angiography Image Acquisition and Processing

The AngioVue provides a noninvasive OCT-based method for visualizing the vascular structures of the retina. It uses an 840-nm light source and has an A-scan rate of 70,000 scans/s and a bandwidth of 50 nm. Each volume contains 304 × 304 A-scans with two consecutive B-scans captured at each fixed position. Each volume scan is acquired in 3 seconds and consists of two orthogonal volumes that are used to minimize motion artifacts arising from microsaccades and fixation changes. The split-spectrum amplitude-decorrelation angiography (SSADA) method was used to capture the dynamic motion of the red blood cells and provide a high-resolution 3D visualization of perfused retinal vasculature.[30]

The AngioVue characterizes vascular information at various user-defined retinal layers as a vessel density map and quantitatively as vessel density (%) (Fig. 1). Vessel density was automatically calculated as the proportion of measured area occupied by flowing blood vessels defined as pixels having decorrelation values acquired by the SSADA algorithm above the threshold level.

For this report, we analyzed vessel density in the peripapillary RNFL in images with a 4.5 × 4.5-mm field of view centered on the optic disc. Vessel density within the RNFL was measured from internal limiting membrane (ILM) to RNFL posterior boundary using standard AngioVue software (version 2015.1.0.90). Measurements were obtained in two areas. Whole enface image vessel density (wiVD) was measured in the entire 4.5 × 4.5-mm image, and circumpapillary vessel density (cpVD) was calculated in the region defined as a 750-μm-wide elliptical annulus extending from the optic disc boundary (Fig. 1).

Image quality review was completed on all scans according to a standard protocol established by the University of California, San Diego Imaging Data Evaluation and Analysis (IDEA) Reading Center. Trained graders reviewed scans and excluded poor quality images, defined as images with (1) a signal strength index of less than 48, (2) poor clarity, (3) residual motion artifacts visible as irregular vessel pattern or disc boundary on the enface angiogram, (4) local weak signal, or (5) RNFL segmentation errors. The location of the disc margin was reviewed for accuracy and adjusted manually if required.

Spectral-Domain OCT Imaging

All subjects also underwent optic nerve head imaging with a commercially available SD-OCT system (Avanti) with a70-kHz axial line rate, 840-nm central wavelength, a 22-μm focal spot diameter, and an axial resolution of 5 μm in tissue.

The optic nerve head (ONH) map protocol was used to obtain RNFL thickness measurements; RNFL measurements were calculated in a 10-pixel-wide band along a circle of 3.45 mm in diameter centered on the ONH. Only good-quality images, as defined by scans with a signal strength index ≥37, and without segmentation failure and artifacts were included. The overall average RNFL thickness was used in this analysis.

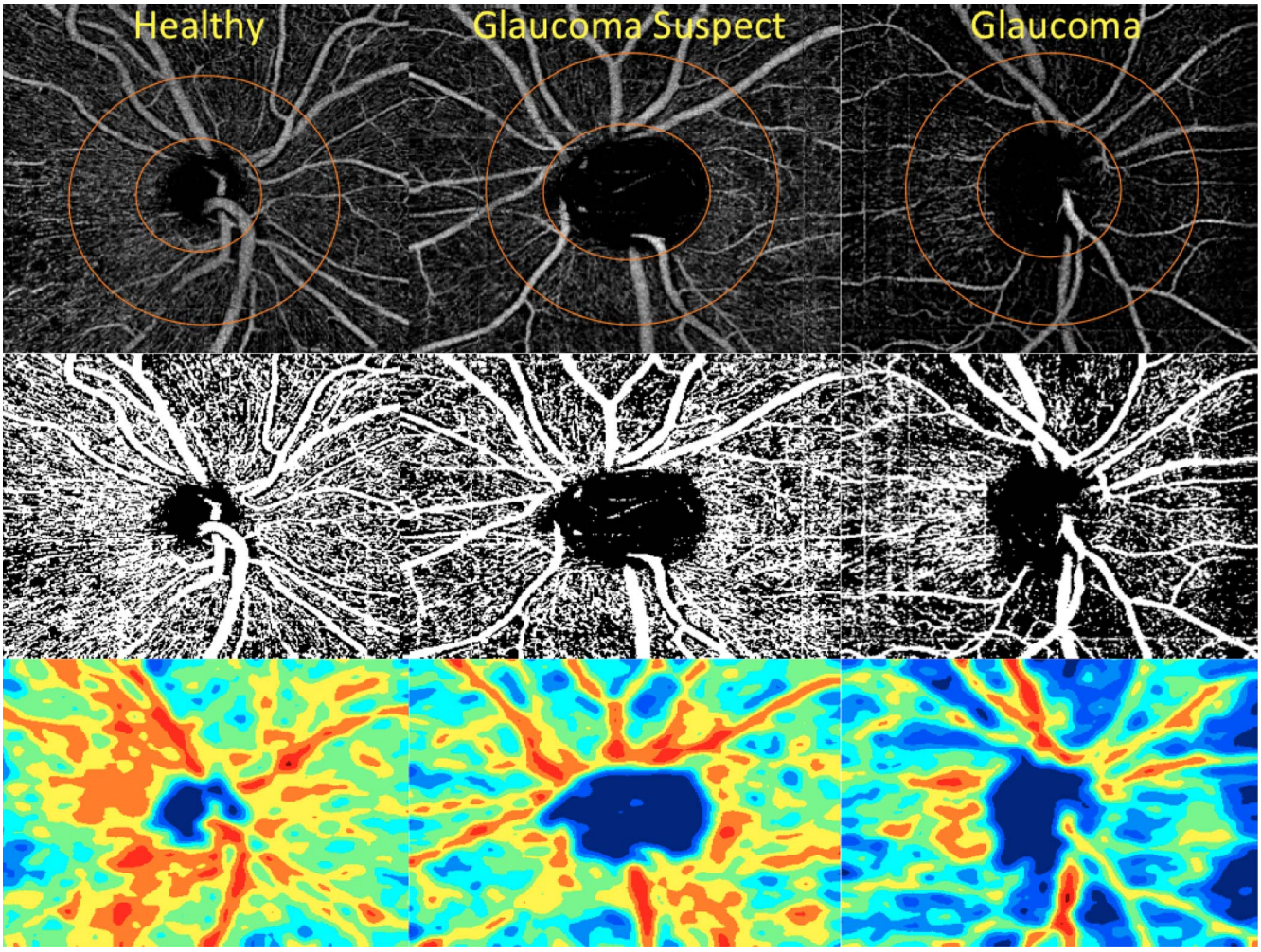

FIGURE 1. Retinal nerve fiber layer vessel density map in healthy, glaucoma suspect, and open-angle glaucoma eyes. *Top row*: circumpapillary vessel density map measurement region defined. *Middle row*: vessel density extracted map overlay on the major retinal vessels. *Bottom row*: area vessel density color-coded map.

Statistical Analysis

The distribution of numerical data was tested for normality using the Shapiro-Wilk test. Descriptive statistics were calculated as the mean and standard deviation for normally distributed variables and median, first quartile, and third quartile for nonnormally distributed variables. Categorical variables were compared using the χ^2 test. Age-adjusted ANOVA was used for the comparison between groups, and the Tukey-Kramer honest significant difference (HSD) post hoc test was performed to adjust for multiple comparisons between groups within each analysis.

Diagnostic accuracy for differentiating between (1) healthy and glaucoma eyes and (2) healthy and glaucoma suspect eyes was evaluated by calculating the area under the receiver operating characteristic (AUROC) curves. For the analysis of vessel density, each participant contributed eyes to either the glaucoma patient group or the glaucoma suspect group, but not both. If both eyes of a glaucoma patient did not show evidence of repeatable visual field damage, then the eye without visual field damage was excluded from the analyses of both the glaucoma eyes and glaucoma suspect eyes.

For completeness, diagnostic accuracy also was calculated for differentiating between (1) healthy subjects and glaucoma patients and (2) healthy subjects and glaucoma suspect participants using the mean vessel density of both eyes as the unit of analysis for each subject.

The AUROC curves were adjusted for age differences between groups, using a covariate adjustment regression method.[36,37] For the analysis by eye, a between-cluster variance estimator was used to adjust for including both eyes of the same subject in the model.

Pairwise comparisons of the AUROCs were performed using the method suggested by Pepe al.[36] to evaluate whether there were statistically significant differences between the ROC curves. All statistical analyses were performed with commercially available software a Stata version 14 (StataCorp, College Station, TX, USA) and JMP version 11.2.0 (SAS, Inc., Cary, NC, USA). The α level (type I error) was set at 0.05 for all comparisons.

RESULTS

Two hundred sixty-one eyes of 164 healthy subjects, glaucoma suspects, and OAG patients with good-quality scans were included in the analysis. Mean age in the healthy group was significantly lower than both glaucoma and glaucoma suspect group ($P < 0.001$; Table 1). Therefore, all comparisons and ROC curves were adjusted for age differences between groups. Compared with glaucoma suspect and healthy subjects,

Table 1. Demographic and Ocular Characteristics of Healthy Subjects, Glaucoma Suspects, and Glaucoma Patients

Variables	Healthy, $n = 23$	Glaucoma Suspect, $n = 37$	Glaucoma, $n = 104$	*P* Value
Demographic characteristics				
Age, y†	53.5 (47.8, 60.2)	68.2 (61.7, 76.3)	72.4 (64.7, 80.8)	<0.001*
Sex, male/female	14/9	23/14	55/49	0.546
Ethnicity, AD/ED	7/16	11/26	28/76	0.913
Clinical characteristics				
Systolic blood pressure, mm Hg†	123.5 (108.8, 138.5)	123.0 (115.5, 136.0)	126.5 (117.0, 136.8)	0.401
Diastolic blood pressure, mm Hg†	79.5 (68.0, 89.5)	79.0 (72.0, 88.0)	77.0 (70.0, 83.0)	0.416
Mean blood pressure, mm Hg‡	95.0 ± 13.5	94.4 ± 10.0	94.4 ± 11.0	0.973
MOPP, mm Hg‡	52.9 ± 8.9	52.0 ± 7.5	54.1 ± 7.5	0.328
Heart rate, beats/min‡	71.0 ± 10.0	69.0 ± 11.2	67.0 ± 11.8	0.333
Self-reported history of diabetes, *n* (%)	1 (4.4%)	5 (13.5%)	15 (14.4%)	0.339
Self-reported history of hypertension, *n* (%)	5 (21.7%)	20 (55.0%)	60 (57.7%)	0.006*
Diabetes medications, *n* (%)	1 (4.4%)	1 (2.7%)	10 (9.6%)	0.321
Antihypertensive medications, *n* (%)	4 (17.4%)	12 (32.4%)	47 (45.2%)	0.011*
Topical glaucoma medications, *n* (%)	0 (0.0%)	27 (73.0%)	87 (83.7%)	<0.001*
Ocular characteristics (mean of both eyes is reported)				
IOP, mm Hg*†	15.5 (13.5, 18.0)	15.5 (13.0, 20.8)	14.0 (11.0, 16.0)	<0.001*
CCT, μm*‡	544.2 ± 38.5	549.4 ± 43.4	530.6 ± 37.8	0.035*
Disc area, mm^2†	1.9 (1.6, 2.2)	1.9 (1.8, 2.5)	2.0 (1.7, 2.4)	0.445
Rim area, mm^2‡	1.3 ± 0.3	1.1 ± 0.3	0.8 ± 0.3	<0.001*
Visual field mean deviation, dB†	0.2 (−0.3, 0.7)	−0.4 (−1.2, 0.1)	−3.9 (−8.8, −1.8)	<0.001*
Visual field pattern standard deviation, dB†	1.5 (1.3, 1.8)	1.8 (1.5, 2.3)	4.6 (2.7, 8.9)	<0.001*

AD, African descent; ED, European descent; MOPP, mean ocular perfusion pressure; IOP, intraocular pressure; CCT, central corneal thickness.

* Statistical significance tested by ANOVA for normal distributions and Kruskal-Wallis tests for nonnormal distributions, all comparisons were corrected with post hoc test.

† Nonnormally distributed variables; represented by median (interquartile range).

‡ Normally distributed variables; represented by mean (±SD).

glaucoma patients had significantly lower IOPs ($P < 0.001$ and $P = 0.042$, respectively), and they had also thinner central corneas compared with the glaucoma suspect group ($P = 0.040$).

There were no statistically significant differences between systolic, diastolic, mean BP and mean ocular perfusion pressure measurements among groups. However, self-reported history of hypertension was more frequent in glaucoma patients and glaucoma suspects compared with healthy controls ($P = 0.006$).

Statistically significant differences were found between glaucoma patients and healthy subjects for all ocular parameters except for disc area. Visual field mean deviation and PSD were not significantly different between glaucoma suspects and healthy controls ($P = 0.819$ and $P = 0.870$, respectively). However, glaucoma suspects had on average thinner RNFL and smaller rim areas compared with healthy subjects ($P < 0.05$ for both).

Age-adjusted 1-way ANOVAs showed that the vessel density values were significantly different among the three groups ($P < 0.001$ for both wiVD and cpVD). The wiVD values were significantly lower in glaucoma eyes (46.2%), followed by glaucoma suspect eyes (51.3%) and healthy eyes (56.6%); all three pairwise comparisons were statistically significant (Tukey-Kramer HSD, $P < 0.05$ for all comparisons). For cpVD, the pairwise comparisons showed that glaucoma eyes (55.1%) had significantly lower cpVD values compared with both glaucoma suspects eyes (60.3%) and healthy eyes (64.2%) (Tukey-Kramer HSD, $P < 0.001$ for both). However, there was

Table 2. Age-Adjusted Mean Values and Diagnostic Accuracy (AUROC) for OCT-A Vessel Density and Spectral-Domain OCT RNFL Thickness Measurements in Healthy Participants, Glaucoma Suspects, and Glaucoma Patients

Diagnostic Parameters	Healthy Eyes Mean (95% CI), $n = 44$	Glaucoma Suspect Eyes Mean (95% CI), $n = 55$	Glaucoma Eyes Mean (95% CI), $n = 124$	*P* Value	AUROC (SE) Glaucoma Eyes Versus Healthy Eyes	AUROC (SE) Glaucoma Suspect Eyes Versus Healthy Eyes
OCT-A whole image vessel density, %	56.6 (55.7–57.4)	51.3 (50.0–52.6)	46.2 (45.2–47.2)	<0.001*†‡§	0.94 (0.03)	0.70 (0.10)
OCT-A circumpapillary vessel density, %	64.2 (63.2–65.2)	60.3 (59.1–61.6)	55.1 (54.0–56.3)	<0.001*†§	0.83 (0.06)	0.65 (0.10)
SD-OCT average RNFL thickness, μm	99.4 (96.3–102.4)	88.4 (84.9–91.8)	74.5 (72.1–76.9)	<0.001*†‡§	0.92 (0.03)	0.65 (0.09)

* Statistical significance tested by ANOVA, corrected with post hoc test.

† Significant difference between mean values of glaucoma and healthy subjects.

‡ Significant difference between mean values of glaucoma suspect and healthy subjects.

§ Significant difference between mean values of glaucoma and glaucoma suspect subjects.

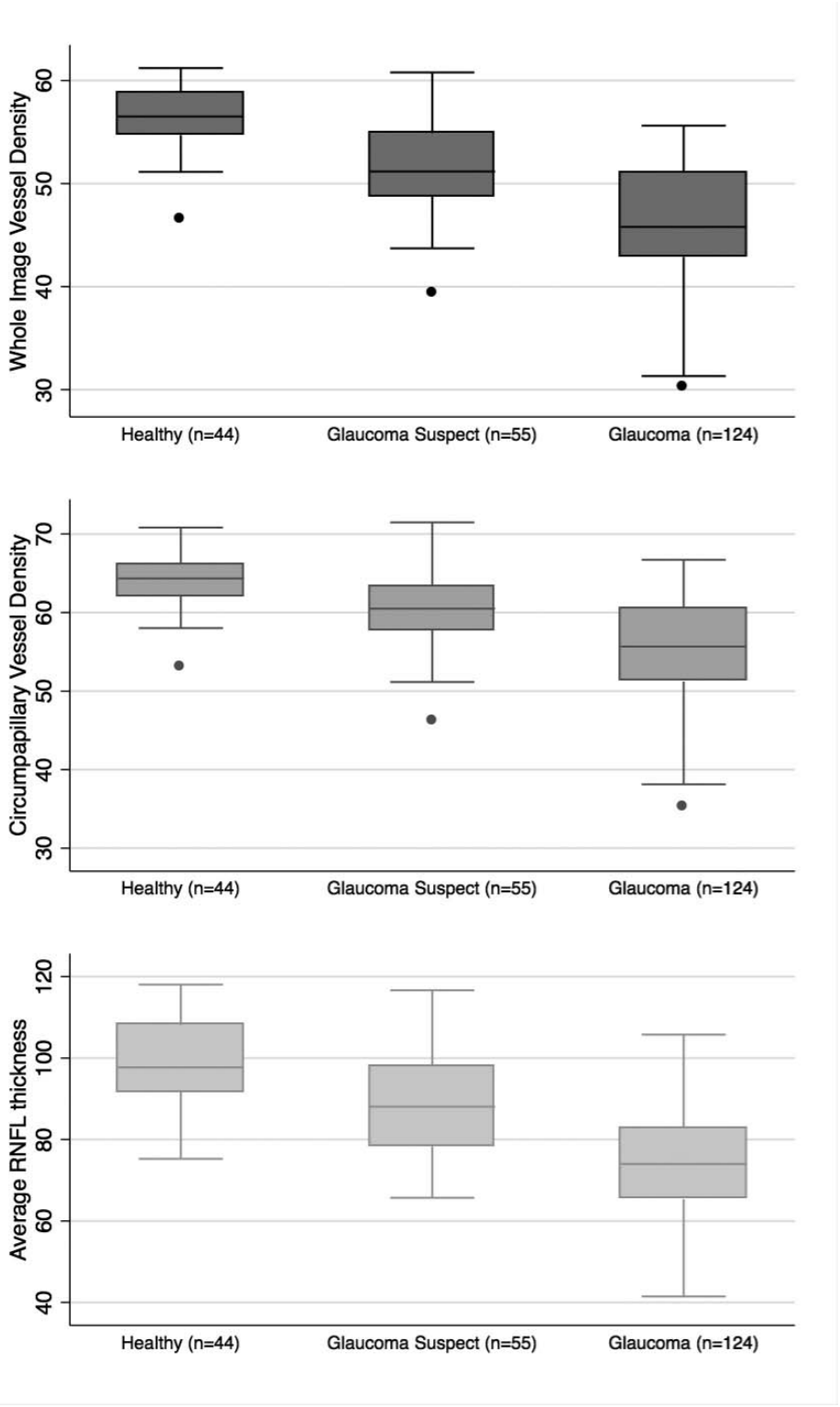

Figure 2. Boxplots illustrating the distribution of whole image vessel density (*top*), circumpapillary vessel density (*middle*), and average retinal nerve fiber layer thickness (*bottom*) measurements in healthy, glaucoma suspect, and glaucoma eyes. The medians are represented by horizontal line in the gray box. *Error bars* denote interquartile range.

no significant difference in cpVD between glaucoma suspect and healthy eyes ($P = 0.426$; Table 2; Fig. 2).

Overall, the AUROC ± SE for discriminating between healthy and glaucomatous eyes was highest for wiVD (0.94 ± 0.03), followed by RNFL (0.92 ± 0.03) and cpVD (0.83 ± 0.06). Pairwise comparisons showed that the age-adjusted AUROC of wiVD (0.94) was higher than cpVD (0.83) ($P < 0.05$), and their diagnostic accuracies were similar to RNFL thickness (0.92) ($P > 0.05$ for both) for differentiating between glaucoma and healthy eyes (Table 2; Fig. 3). The AUROC for differentiating between

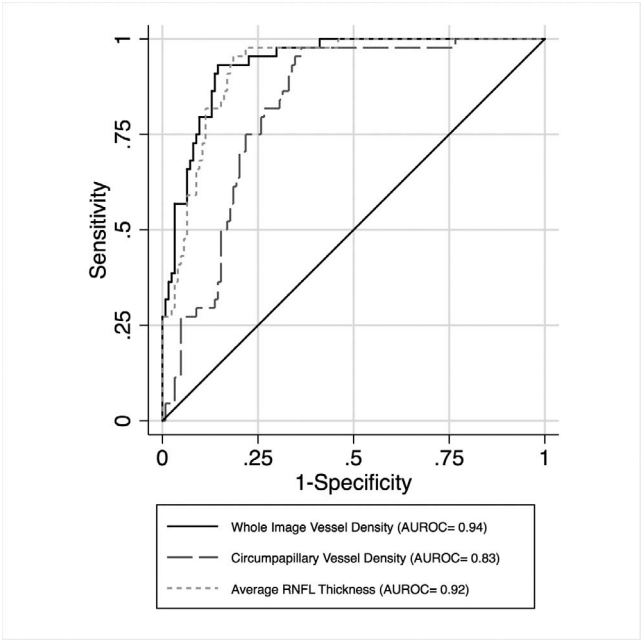

FIGURE 3. Area under the receiver operator characteristic curves for whole image vessel density (0.94), circumpapillary vessel density (0.83), and average RNFL (0.92), for differentiating between glaucoma eyes and healthy eyes.

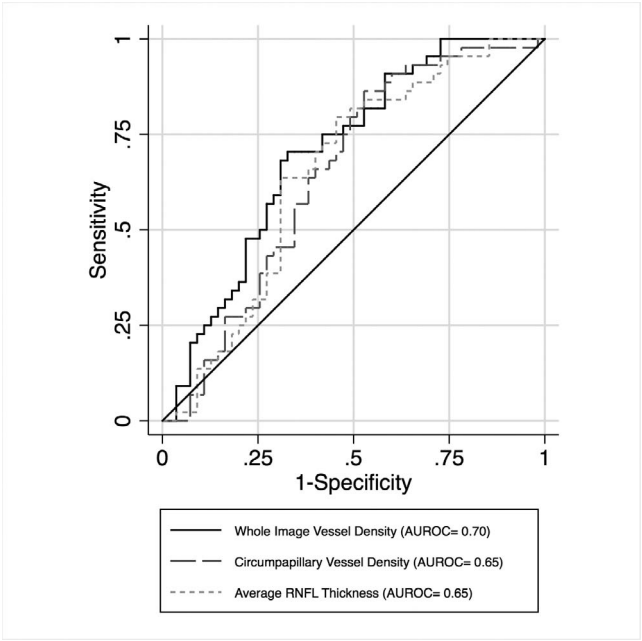

FIGURE 4. Area under the receiver operator characteristic curves for whole image vessel density (0.70), circumpapillary vessel density (0.65), and average RNFL (0.65) for differentiating between glaucoma suspect eyes and healthy eyes.

glaucoma suspect eyes from healthy eyes was highest for wiVD (0.70 ± 0.10), followed by RNFL thickness (0.65 ± 0.09) and cpVD (0.65 ± 0.10). These differences in AUROC did not reach statistical significance (Table 2; Fig. 4).

Similar analyses were completed comparing healthy subjects and glaucoma patients and healthy subjects and glaucoma suspect patients using the mean of both eyes in the analysis. Overall, the AUROC ± SE for discriminating between healthy and glaucomatous participants was highest for wiVD (0.87 ± 0.05), followed by RNFL thickness (0.87 ± 0.04) and cpVD (0.71 ± 0.08). The AUROC for differentiating between healthy and glaucoma suspects was highest for wiVD (0.70 ± 0.11), followed by cpVD (0.62 ± 0.10) and RNFL thickness (0.62 ± 0.09).

DISCUSSION

In the current study, we demonstrated that OCT-A vessel density measured in the RNFL, the most superficial layer of the retina, distinguishes among groups of glaucoma, glaucoma suspect, and healthy participants. Specifically, wiVD performs as well as RNFL thickness for discriminating between healthy and glaucoma patients and for differentiating between the healthy and glaucoma suspect groups. The wiVD also had significantly better diagnostic accuracy than cpVD for differentiating between glaucoma patients and healthy groups.

In the present study, the diagnostic accuracy of vessel density measurements were evaluated for differentiating glaucoma eyes from healthy eyes, as well as glaucoma patients from healthy subjects. Regardless of whether the analysis was completed with the participant as the unit of analysis or whether the eye was the unit of analysis, the same conclusion was drawn; vessel density measures have similar diagnostic accuracy as RNFL thickness for glaucoma and glaucoma suspect detection. However, compared with the analysis with participant as the unit of analysis, the AUROC with eyes as the unit of analysis had larger AUROC values (0.87 and 0.94, respectively) because the analysis by participant included the mean of both eyes in the analysis, regardless of whether the fellow eye had visual field damage.

These results are consistent with previous reports that showed differences in OCT-A microvasculature between glaucoma and healthy groups in the optic disc[31,34] and peripapillary region.[33] However, these reports assessed both the superficial and deep capillary beds and calculated the vascular parameters in a thicker retinal slab from the ILM to the RPE. To our knowledge, this is the first study using OCT-A to evaluate the microvascular bed in the RNFL layer, which largely reflects the RPCs.

These findings that OCT-A vessel density measurements and OCT-based RNFL thickness measurements have a similar AUROC for glaucoma detection are also consistent with other studies reporting high AUROC for both peripapillary vessel density measures in a thicker slab from ILM to RPE and SD-OCT RNFL thickness measurements (AUROCs, 0.94 and 0.97, respectively).[33]

Although structural measurements, such as RNFL and optic nerve head parameters (rim, cup, etc.), have been shown to be associated with disc size,[38] to the best of our knowledge, no studies evaluated the effect of disc size on vessel density measurements. In the current study, there was no significant correlation between disc area and wiVD and cpVD measurements in healthy eyes ($r = 0.04$, $P = 0.815$ and $r = 0.01$, $P = 0.474$, respectively). For this reason, disc area was not controlled for in the analyses.

In the current study, it also was found that wiVD performs as well as RNFL thickness for discriminating between glaucoma suspect eyes and healthy controls, with AUROCs ± SE of 0.70 ± 0.10 and 0.65 ± 0.09, respectively ($P = 0.497$). There is evidence that RNFL thinning is detectable in ocular hypertensive eyes[39,40] and preperimetric glaucomatous eyes[41] even before morphologic changes of the optic disc become visible and visual field defects occur. There is also evidence that changes in the blood flow are detectable in glaucoma suspects with no visual field defect.[42] However, the ability of OCT-A to

discriminate between glaucoma suspects and healthy subjects has not been reported previously.

An unexpected finding in the current study was the significantly better diagnostic accuracy of wiVD compared with cpVD for differentiating between healthy and glaucoma groups. There are several possible explanations for this result. First, the larger measurement area has the advantage of detecting changes in the RPCs, the RNFL capillary plexus, which is an additional superficial vascular bed accompanying axons that extend eccentrically along the temporal vessels.[43] In contrast to RNFL thickness assessment that measures virtually all ganglion cell axons as they exit the eye at the optic nerve, measuring cpVD may not fully capture the presence of most of the RPCs. In this regard, there is no consensus on their origin. Some studies suggest that RPCs originate from retinal vessels in the ganglion cell layer and arch up abruptly to supply the RNFL,[44] whereas others report that they originate from the optic disc.[43] There is, however, consensus regarding the anatomy of the RPCs; these distinct elongated microvascular networks run parallel to the RGC axons and are more prominent in the peripheral arcuate RNFL region.[45] Therefore, the larger measurement area of the wiVD may, at least in part, explain the better performance of these measurements compared to cpVD. As suggested in Figure 1, vessel dropout is visible qualitatively in all areas of the image, including the periphery outside the measurement area of cpVD. Thus, the limited measurement size of cpVD may not include regions of sparse vasculature that are of diagnostic value.

Finally, because the study population comprises a high proportion of early glaucoma patients, the larger measurement area may be detecting early vessel dropout associated with focal RNFL damage in early glaucoma that is more apparent in the peripapillary retina farther from the circumpapillary region included in cpVD.[46]

Impairment of blood flow in the optic nerve and peripapillary retina in glaucoma patients is well documented.[16,18] However, not all studies found significant differences in the blood flow of the neuroretinal rim[47] and peripapillary area[12,48,49] between glaucoma patients and healthy controls. Results of studies relating ocular blood flow to glaucoma are difficult to compare due to the variety of techniques applied, different parameters of ocular hemodynamics investigated, and differences in glaucoma populations studied.

Measurement of ocular blood flow has been challenging, and it should be noted that OCT-A does not directly measure blood flow. A number of methods have been used to document differences in blood flow between glaucoma and normal eyes, but none have been appropriate for routine clinical use.[20] The high variability of Doppler flowmetry and laser speckle flowgraphy measurements,[33,50] the limited resolution with MRI, and invasive nature and time intensiveness of fluorescein angiography[4,6,51] limit their ability to provide information on vascular components that contribute to the pathophysiology of glaucoma.

Doppler OCT[52] has been used for measuring total retinal blood flow, with a better level of precision than other Doppler methods.[53] However, this technique is only able to assess flow in larger retinal vessels and does not provide information on the microvascular networks, which is of primary interest in glaucoma.[34]

The RNFL is largely comprised of the axons of RGCs, one of the most metabolically active cells in human.[54] These cells have tremendous metabolic requirements and depend on regional capillary networks to meet them. Despite the critical role of RNFL capillary plexus relative to glaucomatous damage suggested by several investigators,[21,25,27,55] our previous inability to quantify microvascular network features[29] has prevented evaluation of the clinical characteristics of the RNFL capillary beds and obtaining a more comprehensive understanding of the RGC axonal damage in glaucoma. Based on the results of the current study, we hypothesize that OCT-A provides a new imaging target for early diagnosis and management of glaucoma. Clearly, longitudinal data are needed to evaluate this possibility.

There are several limitations to the current study. First, the healthy participants were significantly younger than the glaucoma suspects and glaucoma patients. For this reason, all analyses were adjusted for age. Moreover, it is unlikely that the main finding that vessel density measures performed as well as RNFL thickness for differentiating between healthy and glaucoma participants would be affected by the age of the healthy controls, as the same subjects are used in all analyses. In addition, due to the cross-sectional, noninterventional design of the study, it was not possible to evaluate the potentially confounding impact of ocular hypotensive eye drops and BP-lowering medications on vascular measurements. Most participants in the glaucoma (83.7%) and glaucoma suspect (73.0%) groups were treated using ocular antihypertensive medications at the time of OCT-A imaging. Further, 41.3% of glaucoma patients and 35.2% glaucoma suspects were taking multiple ocular antihypertensive medications. It also should be noted that in the present study patients were not excluded based on systemic conditions or systemic medication in order to better reflect the general population. As outlined in Table 1, 45.2% of glaucoma patients, 32.4% of glaucoma suspects, and 17.4% of healthy participants with self-reported history of hypertension were taking antihypertensive medications. Therefore, we could not rule out the impact of systemic conditions and systemic medications on vessel density measurements. Further studies are needed to address the influence on OCT-A measurements of ocular hypotensive treatment and systemic medications more specifically. Finally, it was not possible to characterize the causal relationship between altered vessel density and glaucomatous damage. Therefore, longitudinal studies are needed to elucidate the temporal relationship between retinal vascular change and glaucomatous optic neuropathy.

The current study demonstrated that OCT-A vessel density is lower in glaucoma patients compared with healthy controls and glaucoma suspects and has a similar diagnostic accuracy to RNFL thickness for discriminating healthy subjects from glaucoma suspects and glaucoma patients. This study is unique in that it compared the diagnostic accuracy of OCT-A measures and standard SD-OCT RNFL thickness for discriminating between healthy, glaucoma suspect, and glaucoma patients. The ability of OCT-A to noninvasively evaluate the capillary networks shows promise for characterizing glaucomatous retinal vascular changes and may have a role in glaucoma management. Longitudinal studies are needed to determine whether a lower vessel density found in glaucoma patients precedes or follows optic nerve damage and whether this information can be used to improve glaucoma management.

Acknowledgments

Disclosure: **A. Yarmohammadi**, None; **L.M. Zangwill**, Carl Zeiss Meditec (F, R), Heidelberg Engineering (F), National Eye Institute (F), Optovue (F, R), Topcon Medical Systems (F), Quark (F); **A. Diniz-Filho**, None; **M.H. Suh**, None; **P.I. Manalastas**, None; **N. Fatehee**, None; **S. Yousefi**, None; **A. Belghith**, None; **L.J. Saunders,** None; **F.A. Medeiros**, Carl Zeiss Meditec (C, F, R), Heidelberg Engineering (C, F), Topcon (F), Ametek (C, F), Bausch&Lomb (F), Allergan (C, F), Sensimed (F), Alcon (C, F), Merck (F), Reichert (F), National Eye Institute (F), Novartis (C); **D. Huang**, Optovue (C, F, I, R), Carl Zeiss Meditec, (C);P; **R.N.**

Weinreb, Heidelberg Engineering (F), Carl Zeiss Meditec (C, F, R), Genentech (F), Konan (F), National Eye Institute (F), Neurovision (F), Optos (F), Optovue (F), Quark (F), Reichert (F), Topcon (C, F), Alcon (C), Allergan (C), Bausch&Lomb (C), Forsight (C), Valeant (C)

References

1. Weinreb RN, Aung T, Medeiros FA. The pathophysiology and treatment of glaucoma: a review. *JAMA*. 2014;311:1901–1911.
2. Flammer J. The vascular concept of glaucoma. *Surv Ophthalmol*. 1994;38(suppl):S3–S6.
3. Bonomi L, Marchini G, Marraffa M, et al. Vascular risk factors for primary open angle glaucoma: The Egna-Neumarkt Study. *Ophthalmology*. 2000;107:1287–1293.
4. Hitchings RA, Spaeth GL. Fluorescein angiography in chronic simple and low-tension glaucoma. *Br J Ophthalmol*. 1977;61:126–132.
5. Ulrich A, Ulrich C, Barth T, Ulrich WD. Detection of disturbed autoregulation of the peripapillary choroid in primary open angle glaucoma. *Ophthalmic Surg Lasers*. 1996;27:746–757.
6. Spaeth GL. Fluorescein angiography: its contributions towards understanding the mechanisms of visual loss in glaucoma. *Trans Am Ophthalmol Soc*. 1975;73:491–553.
7. Rojanapongpun P, Drance SM. Velocity of ophthalmic arterial flow recorded by Doppler ultrasound in normal subjects. *Am J Ophthalmol*. 1993;115:174–180.
8. Weinreb RN, Bartsch DU, Freeman WR. Angiography of the glaucomatous optic nerve head. *J Glaucoma*. 1994;3(suppl 1):S55–S60.
9. Hamard P, Hamard H, Dufaux J, Quesnot S. Optic nerve head blood flow using a laser Doppler velocimeter and haemorheology in primary open angle glaucoma and normal pressure glaucoma. *Br J Ophthalmol*. 1994;78:449–453.
10. Weinreb RN, Harris A, eds. *Ocular Blood Flow in Glaucoma*. Amsterdam, The Netherlands: Kugler Publications; 2009.
11. Harris A, Kagemann L, Cioffi GA. Assessment of human ocular hemodynamics. *Surv Ophthalmol*. 1998;42:509–533.
12. Tobe LA, Harris A, Hussain RM, et al. The role of retrobulbar and retinal circulation on optic nerve head and retinal nerve fibre layer structure in patients with open-angle glaucoma over an 18-month period. *Br J Ophthalmol*. 2015;99:609–612.
13. Jonas JB, Nguyen XN, Naumann GO. Parapapillary retinal vessel diameter in normal and glaucoma eyes. I. Morphometric data. *Invest Ophthalmol Vis Sci*. 1989;30:1599–1603.
14. Jonas JB, Nguyen XN, Gusek GC, Naumann GO. Parapapillary chorioretinal atrophy in normal and glaucoma eyes. I. Morphometric data. *Invest Ophthalmol Vis Sci*. 1989;30:908–918.
15. Banitt M. The choroid in glaucoma. *Curr Opin Ophthalmol*. 2013;24:125–129.
16. Flammer J, Orgul S. Optic nerve blood-flow abnormalities in glaucoma. *Prog Retin Eye Res*. 1998;17:267–289.
17. Yokoyama Y, Aizawa N, Chiba N, et al. Significant correlations between optic nerve head microcirculation and visual field defects and nerve fiber layer loss in glaucoma patients with myopic glaucomatous disk. *Clin Ophthalmol*. 2011;5:1721–1727.
18. Rankin SJ, Drance SM. Peripapillary focal retinal arteriolar narrowing in open angle glaucoma. *J Glaucoma*. 1996;5:22–28.
19. Michelson G, Langhans MJ, Groh MJ. Perfusion of the juxtapapillary retina and the neuroretinal rim area in primary open angle glaucoma. *J Glaucoma*. 1996;5:91–98.
20. Schuman JS. Measuring blood flow: so what? *JAMA Ophthalmol*. 2015;133:1052–1053.
21. Henkind P. Radial peripapillary capillaries of the retina. I. Anatomy: human and comparative. *Br J Ophthalmol*. 1967;51:115–123.
22. Henkind P, Bellhorn RW, Poll D. Radial peripapillary capillaries. 3. Their development in the cat. *Br J Ophthalmol*. 1973;57:595–599.
23. Ueno H. Studies on the radial peripapillary capillaries (RPCs). (1) Clinical features on fluorescein fundus angiography [in Japanese]. *Nippon Ganka Gakkai Zasshi*. 1976;80:267–280.
24. Liao JS. A study of fluoro-angiographic pattern of the radial peripapillary capillaries [in Chinese]. *Zhonghua Yan Ke Za Zhi*. 1981;17:197–199.
25. Kornzweig AL, Eliasoph I, Feldstein M. Selective atrophy of the radial peripapillary capillaries in chronic glaucoma. *Arch Ophthalmol*. 1968;80:696–702.
26. Alterman M, Henkind P. Radial peripapillary capillaries of the retina. II. Possible role in Bjerrum scotoma. *Br J Ophthalmol*. 1968;52:26–31.
27. Daicker B. Selective atrophy of the radial peripapillary capillaries of the retina and glaucomatous visual fields [in German]. *Ophthalmologica*. 1976;172:138.
28. Yu PK, Cringle SJ, Yu DY. Correlation between the radial peripapillary capillaries and the retinal nerve fibre layer in the normal human retina. *Exp Eye Res*. 2014;129:83–92.
29. Yu PK, Balaratnasingam C, Xu J, et al. Label-free density measurements of radial peripapillary capillaries in the human retina. *PLoS One*. 2015;10:e0135151.
30. Jia Y, Tan O, Tokayer J, et al. Split-spectrum amplitude-decorrelation angiography with optical coherence tomography. *Opt Express*. 2012;20:4710–4725.
31. Jia Y, Wei E, Wang X, et al. Optical coherence tomography angiography of optic disc perfusion in glaucoma. *Ophthalmology*. 2014;121:1322–1332.
32. Wang X, Jiang C, Ko T, et al. Correlation between optic disc perfusion and glaucomatous severity in patients with open-angle glaucoma: an optical coherence tomography angiography study. *Graefes Arch Clin Exp Ophthalmol*. 2015;253:1557–1564.
33. Liu L, Jia Y, Takusagawa HL, et al. Optical coherence tomography angiography of the peripapillary retina in glaucoma. *JAMA Ophthalmol*. 2015;133:1045–1052.
34. Jia Y, Morrison JC, Tokayer J, et al. Quantitative OCT angiography of optic nerve head blood flow. *Biomed Opt Express*. 2012;3:3127–3137.
35. Sample PA, Girkin CA, Zangwill LM, et al. The African Descent and Glaucoma Evaluation Study (ADAGES): design and baseline data. *Arch Ophthalmol*. 2009;127:1136–1145.
36. Pepe M, Longton G, Janes H. Estimation and comparison of receiver operating characteristic curves. *Stata J*. 2009;9:1–16.
37. Alonzo TA, Pepe MS. Distribution-free ROC analysis using binary regression techniques. *Biostatistics*. 2002;3:421–432.
38. Budenz DL, Anderson DR, Varma R, et al. Determinants of normal retinal nerve fiber layer thickness measured by Stratus OCT. *Ophthalmology*. 2007;114:1046–1052.
39. Gyatsho J, Kaushik S, Gupta A, et al. Retinal nerve fiber layer thickness in normal, ocular hypertensive, and glaucomatous Indian eyes: an optical coherence tomography study. *J Glaucoma*. 2008;17:122–127.
40. Anton A, Moreno-Montanes J, Blazquez F, et al. Usefulness of optical coherence tomography parameters of the optic disc and the retinal nerve fiber layer to differentiate glaucomatous, ocular hypertensive, and normal eyes. *J Glaucoma*. 2007;16:1–8.
41. Lisboa R, Paranhos A Jr, Weinreb RN, et al. Comparison of different spectral domain OCT scanning protocols for diagnosing preperimetric glaucoma. *Invest Ophthalmol Vis Sci*. 2013;54:3417–3425.

42. Michelson G, Langhans MJ, Harazny J, Dichtl A. Visual field defect and perfusion of the juxtapapillary retina and the neuroretinal rim area in primary open-angle glaucoma. *Graefes Arch Clin Exp Ophthalmol*. 1998;236:80–85.
43. Toussaint D, Kuwabara T, Cogan DG. Retinal vascular patterns. II. Human retinal vessels studied in three dimensions. *Arch Ophthalmol*. 1961;65:575–581.
44. Scoles D, Gray DC, Hunter JJ, et al. In-vivo imaging of retinal nerve fiber layer vasculature: imaging histology comparison. *BMC Ophthalmol*. 2009;9:9–17.
45. Chan G, Balaratnasingam C, Xu J, et al. In vivo optical imaging of human retinal capillary networks using speckle variance optical coherence tomography with quantitative clinico-histological correlation. *Microvasc Res*. 2015;100:32–39.
46. Leung CK, Lam S, Weinreb RN, et al. Retinal nerve fiber layer imaging with spectral-domain optical coherence tomography: analysis of the retinal nerve fiber layer map for glaucoma detection. *Ophthalmology*. 2010;117(9):1684–1691.
47. Hollo G, van den Berg TJ, Greve EL. Scanning laser Doppler flowmetry in glaucoma. *Int Ophthalmol*. 1996;20:63–70.
48. Deokule S, Vizzeri G, Boehm A, et al. Association of visual field severity and parapapillary retinal blood flow in open-angle glaucoma. *J Glaucoma*. 2010;19:293–298.
49. Kerr J, Nelson P, O'Brien C. A comparison of ocular blood flow in untreated primary open-angle glaucoma and ocular hypertension. *Am J Ophthalmol*. 1998;126:42–51.
50. Yaoeda K, Shirakashi M, Funaki S, et al. Measurement of microcirculation in the optic nerve head by laser speckle flowgraphy and scanning laser Doppler flowmetry. *Am J Ophthalmol*. 2000;129:734–739.
51. Spaide RF, Klancnik JM Jr, Cooney MJ. Retinal vascular layers imaged by fluorescein angiography and optical coherence tomography angiography. *JAMA Ophthalmol*. 2015;133:45–50.
52. Wang Y, Bower BA, Izatt JA, et al. Retinal blood flow measurement by circumpapillary Fourier domain Doppler optical coherence tomography. *J Biomed Opt*. 2008;13:064003.
53. Hwang JC, Konduru R, Zhang X, et al. Relationship among visual field, blood flow, and neural structure measurements in glaucoma. *Invest Ophthalmol Vis Sci*. 2012;53:3020–3026.
54. Yu DY, Cringle SJ, Balaratnasingam C, et al. Retinal ganglion cells: energetics, compartmentation, axonal transport, cytoskeletons and vulnerability. *Prog Retin Eye Res*. 2013;36:217–246.
55. Henkind P. Symposium on glaucoma: joint meeting with the National Society for the Prevention of Blindness. New observations on the radial peripapillary capillaries. *Invest Ophthalmol Vis Sci*. 1967;6:103–108.

Investigative Ophthalmology & Visual Science